Final Report

August 2009

Low-Cost Substrates for High-Performance Nanorod Array LEDs

Work Performed Under Agreement:
DE-FC26-06NT42862

Submitted By:
Purdue University
Birck Nanotechnology Center
1205 West State Street
West Lafayette, IN 47907-2057

Principal Investigator:
Timothy D. Sands
Phone Number: (765)496-6105
Fax Number: (765)496-8383
E-Mail: tsands@purdue.edu
Co-PIs: Eric A. Stach and R. Edwin García

Submitted To:

U. S. Department of Energy
National Energy Technology Laboratory
Project Officer: Ryan Egidi
E-Mail:Ryan.Egidi@netl.doe.gov

DISCLAIMER

Table of Contents

A. Overview

The completed project, entitled *"Low-Cost Substrates for High-Performance Nanorod LEDs,"* targeted the goal of a phosphor-free nanorod-based white LED with IQE > 50% across the spectrum from 450 nm to 600 nm on metallized silicon substrates. The principal achievements of this project included:

- Demonstration of (In,Ga)N nanopyramid heterostructures by a conventional OMVPE process.
- Verification of complete filtering of threading dislocations to yield dislocation-free pyramidal heterostructures.
- Demonstration of electroluminescence with a peak wavelength of ~600 nm from an (In,Ga)N nanopyramid array LED.
- Development of a reflective ZrN/AlN buffer layer for epitaxial growth of GaN films and GaN nanopyramid arrays on (111)Si.

These achievements are highlighted below.

B. Results

B.1. Selected-Area GaN nanorod and nanopyramid growth: In 2005, Purdue researchers, including Stach and Sands, reported a method for growing GaN nanorod arrays by OMVPE without catalysts and without the need for lithography [Deb05]. The process flow began with the deposition of a SiO_x or SiN_x template on GaN, followed by an aluminum layer of thickness ~1 μm. The Al film was then anodized, stripped of the anodic oxide, and anodized again, resulting in an array of vertical pores with short-range hexagonal order in an anodic alumina mask. Reactive ion etching (RIE) through this mask opened up nanoscale windows in the underlying template. The porous anodic alumina (PAA) mask was then removed and GaN nanorods were grown selectively in the openings of the template by OMVPE. Figure 1 shows a plan-view field-emission scanning electron microscope (FESEM) image along with a cross-sectional transmission electron microscope (TEM) image of the resulting nanorods. The nanorods grown at a temperature of ~1030°C were found to terminate in a pyramidal cap with "semipolar" $\{1\bar{1}01\}$ facets. As determined during the SSL project, the nanorods are free of extended defects, including stacking faults and

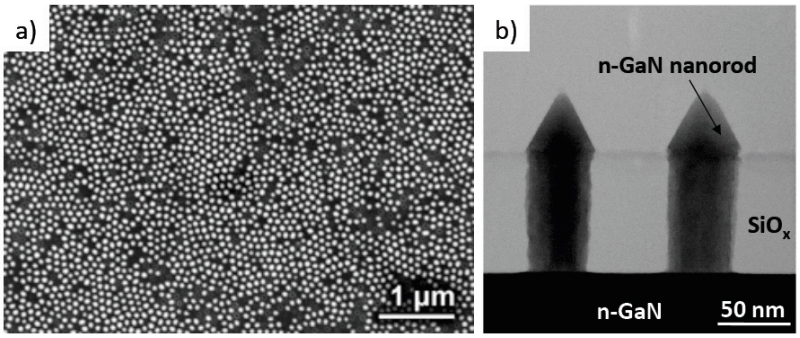

Figure 1 a) – Plan-view FESEM image of GaN nanorod array fabricated by selective growth in a template formed by reactive ion etching through a porous anodic alumina mask; b) Cross-sectional TEM image of adjacent nanorods, showing pyramidal caps.

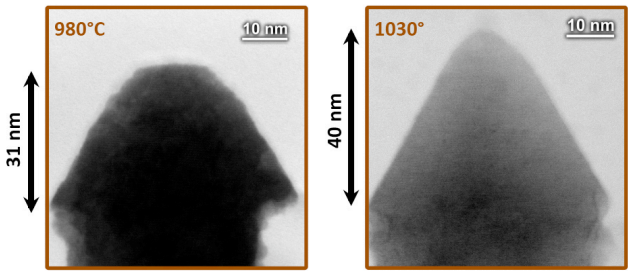

Figure 2 – TEM images of GaN nanorod "seeds" grown at 980°C (left) and 1030°C (right). The shape of the (In,Ga)N layer grown on the pyramidal cap is controlled by the shape of the seed.

zincblende lamellae. The control of the apex shape with growth temperature was also demonstrated, as shown in Figure 2. Control of the apex shape allows control of the volume and shape of the (In,Ga)N apex quantum dot, as will be described below.

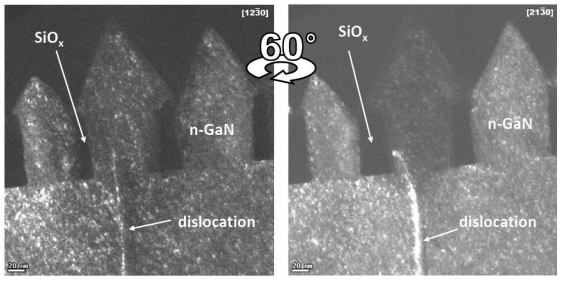

Figure 3 – Cross-sectional weak-beam dark-field TEM images of a "lucky" threading dislocation that enters the base of a GaN nanorod, terminating at the surface of the nanorod. The bend in the dislocation is apparent in the tilted image (right).

B.2. Dislocation filtering: One of the most promising aspects of the nanorod array approach is the potential for significantly reducing the threading dislocation density through a combination of blocking (termination at the interface with the template) and bending (image forces directing dislocations to the free surfaces of the nanorods). During this project, more than 2,500 individual nanorods were analyzed by TEM. All were found to be free of threading dislocations. Although most of the threading dislocations from the underlying GaN layer were blocked, several "lucky" dislocations that were aligned with the template openings were studied, and all turned into the interface at the nanorod base, or penetrated the nanorod by 30 nm at most before bending to the prism face of the nanorod where they terminated. Figure 3 illustrates the latter case. These experimental results were augmented by a continuum modeling approach incorporating the full tensor description of the elastic properties of wurtzite GaN [Colby09]. The models show that the pyramidal cap on the growing nanorod plays an important role in directing the dislocations out of the nanorod. Based on these results and some recent experimental evidence by other groups [Chen09], complete filtering of threading dislocations can be expected in this system up to GaN nanorod diameters of about 250 nm.

B3. Growth of (In,Ga)N on GaN nanopyramids: The growth conditions for (In,Ga)N quantum wells and GaN cladding layers were optimized. Typical growth conditions for the quantum wells were V/III ratio of 7700, growth temperature of 650°C, TMI/TMG ratio of 0.8, total pressure of 100 torr and growth time of 90 seconds. GaN cladding layer growth conditions were V/III ratio of 1630, growth temperature of 715°C, total pressure of 100 torr and growth time of 120 seconds. The cladding layer growth temperature was found to have a significant effect on the growth morphology. Lower temperatures resulted in undesirable nucleation of polycrystalline GaN on the template, whereas higher growth temperatures favored nonuniform growth, with some nanorods showing little overgrowth, while others exhibited explosive growth. For the flow rates and pressures chosen, the growth temperature of 715°C yielded the most uniform results. It is anticipated that a more ordered array of nanorod seeds would yield a wider growth window for the GaN cladding layer.

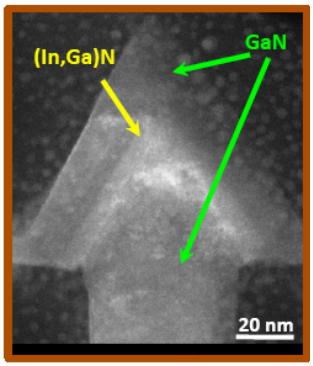

Figure 4 – Dark- field annular- aperture STEM image of a nanorod seed after growth of the (In,Ga)N layer and cladding GaN layer.

Figure 4 shows a scanning transmission electron microscope (STEM) image of a nanorod heterostructure in dark-field annular aperture mode to reveal the "Z contrast" between In and Ga. The nanorod seed in this case was grown at 980°C, yielding a basal facet at the apex as illustrated in Figure 2. The contrast suggests that the InN is distributed both on the semipolar facets and at the apex, with the (In,Ga)N at the apex terminating in a sharp tip. This conclusion is reinforced by the mapping of the energy dispersive analysis of characteristic x-rays (EDS) shown in Figure 5. In this map (obtained at Argonne National Laboratory with the assistance of Dr. Nestor Zaluzec), indium is red, gallium is green and silicon is blue. The overlap of Ga and In signals is revealed as yellow.

Note that these images were obtained in transmission, so the electron beam was exciting characteristic x-rays from all six semipolar facets, as well as the apex quantum dot.

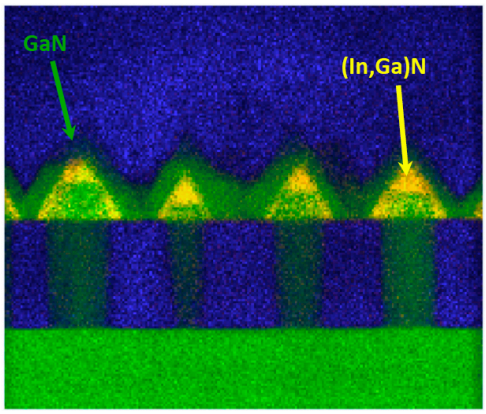

Figure 5 – EDS map of Ga, In and Si in the nanorod/nanopyramid sample imaged in Figure 5. Note that the (In,Ga)N (yellow) covers the semipolar facets and forms a pyramidal cap on the basal facet at the apex of the GaN seed.

Although the GaN nanorod seeds grown at temperatures above ~900°C are free of extended defects including stacking faults, subsequent GaN growth at lower temperatures yields stacking faults such as those shown in Figure 6. These faults initiate at or above the apex of the seed, and they do not terminate in the nanopyramid. Thus, there are no partial dislocations bounding the faults that are retained in the crystal. As these faults appear to be unrelated to strain, they are believed to originate from growth mistakes. Growth of (In,Ga)N, however, can yield both faults and zincblende lamellae (see Figure 7). The appearance of the zincblende phase may be related to the reduction of coherency strain energy, in contrast to the origin of the faults seen in low-temperature GaN growth on GaN nanorod seeds. As in the case of GaN stacking faults, the zincblende inclusions do not terminate in the crystal with partial dislocations. Hence, their impact on device performance is not necessarily detrimental. The band offsets associated with wurtzite/zincblende interfaces are modest [Majewski98], however, the impact of these lamellae on the electric field associated with piezoelectricity and the termination of the spontaneous dipole moment may influence the radiative recombination rate in these (In,Ga)N heterostructures.

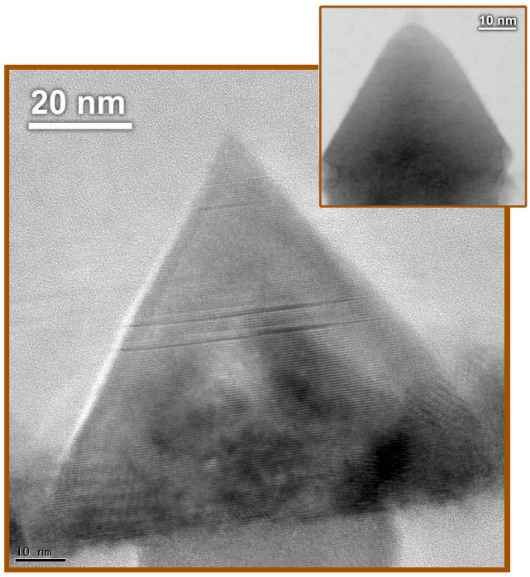

Figure 6 – TEM image showing stacking faults arising during low-temperature growth of GaN on top of a GaN seed (example shown in upper right) that was grown at 1030°C. The stacking faults initiate at the apex of the seed.

B.4. Overgrowth of (In,Ga)N-clad nanopyramids: Growth conditions for the p-GaN hole injection layer were adapted from conditions optimized for planar LEDs in the Purdue OMVPE reactor. These conditions (V/III ratio of 1430, temperature of 1030°C, Cp_2Mg flow of 0.96 nmol/min and total pressure of 100 torr) yielded a hole concentration of ~2 x $10^{17}/cm^3$ in planar films. Figure 8 shows a sequence of FESEM images, the last of which is a low magnification image of the p-GaN layer just before complete coalescence (26 minutes of growth, yielding ~800 nm of p-GaN). Although such heterostructures are suitable for electroluminescent devices, the natural pitch (100-200 nm depending on anodization conditions) of the PAA template forces the impingement of neighboring nanopyramids, as the minimum thickness of p-GaN for suitable hole injection is ~150 nm.

Impingement eliminates the potential geometric advantages of the pyramid geometry for light extraction. Furthermore, the coalescing pyramids result in extended defects arising from the uncorrelated basal faults and zincblende lamellae in adjacent nanopyramids. Some of these defect reactions generate threading dislocations that may have deleterious effects on junction leakage and nanoradiative recombination. Figure 9 includes cross-sectional TEM images of the thick p-GaN layer imaged in Figure 9. Note the threading dislocations that result from nanopyramid impingement. Although these dislocations are present in high density, it may be important that they do not traverse into the (In,Ga)N active region. Nevertheless, an optimal design will likely require non-impinging nanopyramids (see Section C).

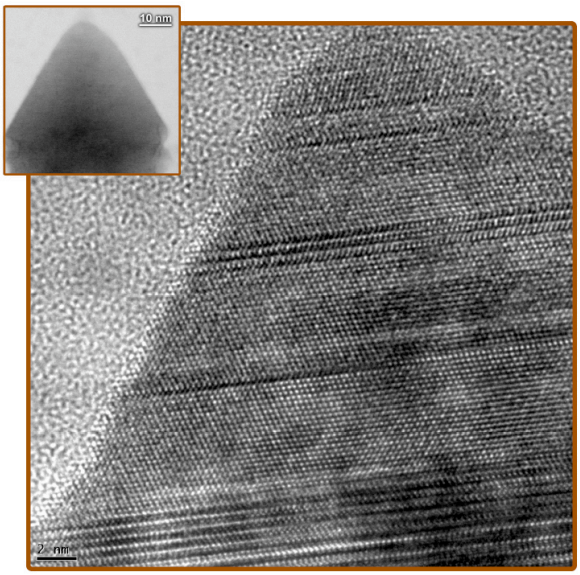

Figure 7 – TEM image of (In,Ga)N-clad GaN seed, showing stacking faults and zincblende lamellae. These defects initiate at the apex of the defect-free (upper left). Note that the same seed wafer was used for the growth runs imaged in Figures 7 and 8.

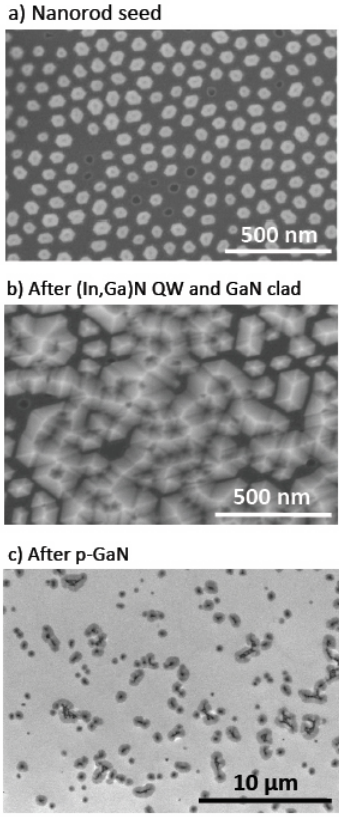

Figure 8 – Sequence of FESEM images at different stages of the growth of a device heterostructure (described in text).

B.5. Modeling of stress and mechanical strain energy distribution: The development of 3D models of the stress distribution and strain energy density in complex nanorod/nanopyramid heterostructures using the full tensor elastic properties of the wurtzite structure of GaN and (In,Ga)N was an important achievement of this project [Liang09]. An example of the results of such calculations is shown in Figure 10. These calculations were used to predict the preferential growth of (In,Ga)N at the apex, rim and facet intersections of the GaN seed, as these are the locations where the strain energy density is lowest and the barrier to desorption of In-containing species is highest. Future work will include the extension of these models to include piezoelectric and pyroelectric effects as the basis for describing the complex electric

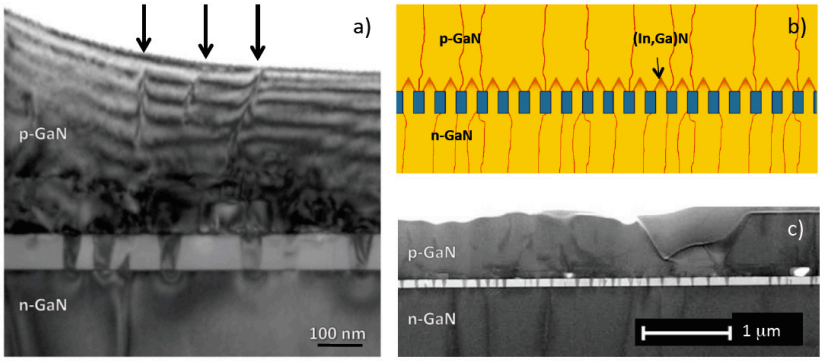

Figure 9 – a) Cross-sectional bright-field TEM image of the sample imaged in Fig. 9c), showing dislocations arising from nanopyramid impingement in the p-GaN layer. A schematic of the sample is shown in b). c) is a lower magnification TEM image.

field distribution in nanopyramid heterostructures.

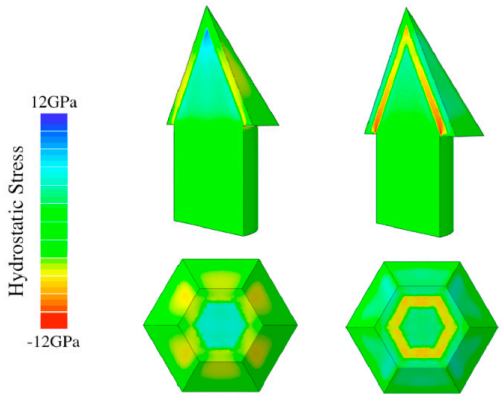

Figure 10 – Magnitude of hydrostatic stress in nanorod/nanopyramid heterostructures. An (In,Ga)N cladding layer on a GaN seed is shown at left. The figures on the right show the stress distribution after adding a GaN cladding layer [Liang09].

B.6. IQE measurement by PL: The heterostructure depicted in Figure 8b (i.e., before growth of the p-GaN) was characterized by temperature dependent PL. The excitation source was a 325 nm HeCd laser operating in the weak excitation regime (~1 Wcm^{-2}), which has been recommended when using the ratio of integrated PL intensity at 300K to that at 4K as an estimation of IQE [Chichibu06]. Figure 11 shows the PL spectrum of the nanopyramid heterostructure at 300K and at 4K. Note that the peak emission wavelength at 300K is 620 nm (red-orange), significantly beyond the target wavelength of 555 nm. The integrated intensity at 300K is 10.3% of the integrated intensity at 4K. As will be discussed below and in Section C, the PL ratio is most likely an overestimate of the IQE. Nevertheless, this is among the highest ratios reported for PL at wavelengths greater than 600 nm, suggesting that the quality of the active region is at least as high as that of state-of-the-art planar orange and red-orange (In,Ga)N LEDs.

An important caveat to this preliminary conclusion is that a thorough and quantitative study of the time decay and temperature dependence of the PL signal is required in order to separate the contributions that may be arising from yellow defect luminescence, which is typically observed in PL of GaN nanorods and nanowires [Wang09]. In the experiments performed at Purdue, nanopyramids grown without quantum wells were found to yield yellow luminescence. However, the temperature dependence of the intensity was weak, as is typical for yellow defect luminescence in GaN [Reshchikov01]. Thus, for accurate IQE measurements, special care must be taken to ensure that the contribution of yellow defect luminescence is not included in the integrated PL intensity at 300K.

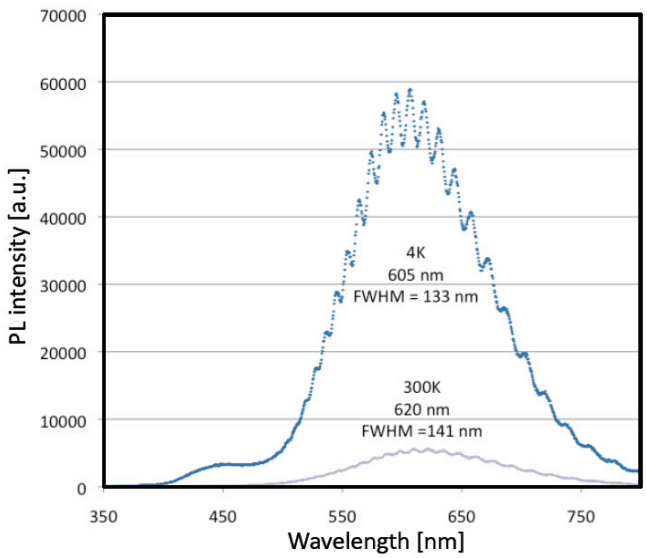

Figure 11 – PL from the nanopyramid array sample imaged in Figure 8b. The PL intensity at 300K is 10.3% of the 4K PL intensity, a promising result given the red-orange peak emission wavelength. The shoulder at 450 nm for the 4K PL is attributed to defect luminescence in the HVPE buffer layer.

B.7. Nanopyramid LEDs: The heterostructure shown in Figures 8c and 9 was patterned, etched and contacted to yield an LED device [Wildeson09a]. The room temperature *cw* EL spectrum is shown in Figure 12. The peak of the emission was at 606 nm (slightly blue-shifted from the PL) and the FWHM was 180 nm (slightly broader than the PL spectrum). The emission wavelength corresponds to an approximate composition of $In_{0.32}Ga_{0.68}N$, although direct measurement of the composition has not yet been achieved. The broad EL and PL peaks may be the result of variations between nanopyramids as evident in Figure 5, as well as differing emission wavelengths from the (In,Ga)N at the apex

and the (In,Ga)N quantum wells on the semipolar facets. Longer emission wavelengths at the apex of microscale pyramids have been observed by other researchers using CL [Pérez-Solórzano05]. Planar LEDs produced during the same growth run as the nanorod LED had a peak EL emission wavelength of 561 nm. The 45 nm red-shift observed when growing quantum wells on nanopyramids as compared to the planar thin film heterostructure further supports the hypothesis that strain relaxation inherent in nanostructures allows greater InN incorporation. In addition, the degree of red-shift in the EL data observed here corresponds well with recent PL data that show a 36 nm red-shift when comparing similar sized nanorod heterostructures to thin film heterostructures that emit within the blue portion of the spectrum [Zang09].

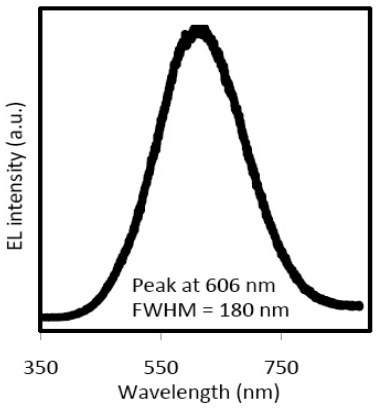

Figure 12 – Room temperature *cw* EL spectrum from nanopyramid array LED [Wildeson09a].

B.8. Metallized silicon substrates for GaN: The effective filtering of dislocations by templated nanorod arrays enables consideration of alternative substrates that might be expected to yield more defective planar GaN epilayers than is typically achieved on sapphire. Thus, a major thrust of the project was the development of a Si-based substrate for GaN nanorod devices. A ZrN/AlN intermediate bilayer on (111)Si was developed as a reflective substrate for growth of nanorod heterostructures [Oliver08]. ZrN is a refractory metal with reflectivity above 80% at wavelengths greater than 500 nm. The AlN layer prevents reactions between ZrN and Si at the OMVPE growth temperature (~1030°C). Figure 13 shows x-ray diffraction patterns from GaN epilayers grown on sapphire and on metallized silicon. The epitaxial quality of these relatively thin epilayers (~800 nm) is comparable. Figure 14 shows a nanopyramid array prepared on the GaN/ZrN/AlN/Si substrate.

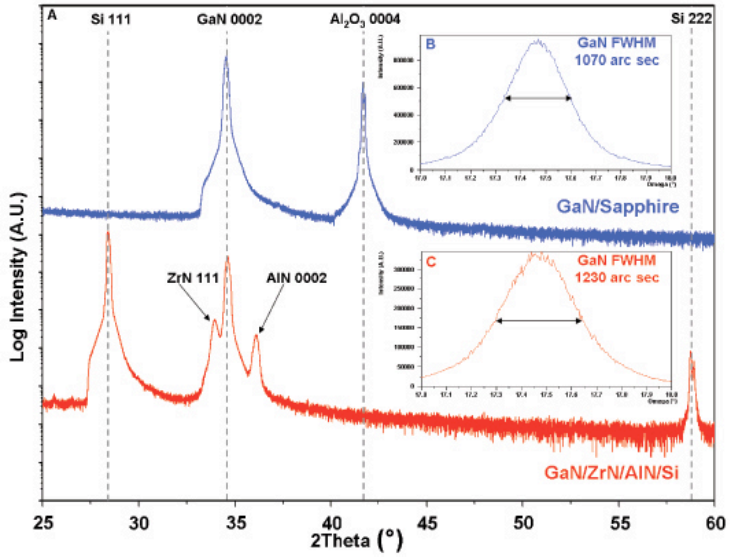

Figure 13 – XRD patterns from GaN grown on sapphire (blue) and ZrN/AlN/Si during the same growth run. Note that the full-width-at-half-maximum of the 0002 reflection is comparable

A provisional patent application covering this metallized silicon substrate invention was converted to a US patent application and PCT on April 15th, 2009. The publication of this work generated substantial worldwide attention from the lay press, trade journals and venture capital communities. Thus far, the PI has discussed licensing with three NGLIA member companies. The PI's students, Isaac Wildeson and Mark Oliver, along with MBA students from Purdue's Krannert School of Management, developed a business plan around the substrate technology, winning the recent Global Venture Challenge at Oak Ridge National Laboratory.

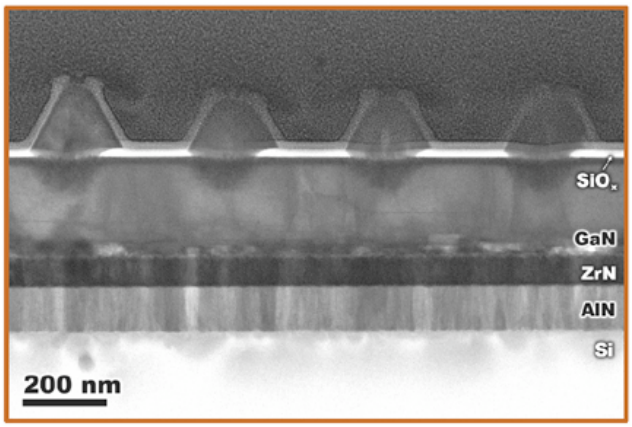

Figure 14 – GaN nanopyramids grown on GaN / ZrN / AlN / (111)Si substrate.

Although the use of metallized silicon as a substrate was motivated by the insensitivity of the nanorod/nanopyramid design to threading dislocations, all LED technologies based on GaN could be impacted by a practical silicon substrate solution, especially if the switch to silicon would reduce the processing and packaging complexity, and hence, the initial cost of high-brightness LEDs. The development of a silicon substrate technology for planar LEDs based on the ZrN/AlN bilayer approach was outside the scope of this SSL project. This effort will be pursued separately in the future.

C. Conclusions and Recommendations for Future Work

Among the important conclusions of the completed project are:

- Nanorod seeds effectively eliminate threading dislocations
- The nanopyramid heterostructures are free of dislocations, although they do contain stacking faults and zincblende inclusions.
- The natural facets of the nanopyramid caps are semipolar, and are therefore expected to result in polarization-induced electric fields that are approximately a factor of 10 lower than those in c-plane quantum wells [Park07]. The reduced electric field in the quantum well is expected to result in a substantial decrease in the degree of efficiency droop as devices are pushed to higher current densities [Zhong07]
- Nanopyramid heterostructures exhibit PL and EL well into the green and beyond. However, extensive characterization of EL and PL as a function of temperature and time will be necessary to separate green (In,Ga)N luminescence from defect luminescence, a necessary step in order to establish a baseline for improving the IQE in the 540-560 nm wavelength range.

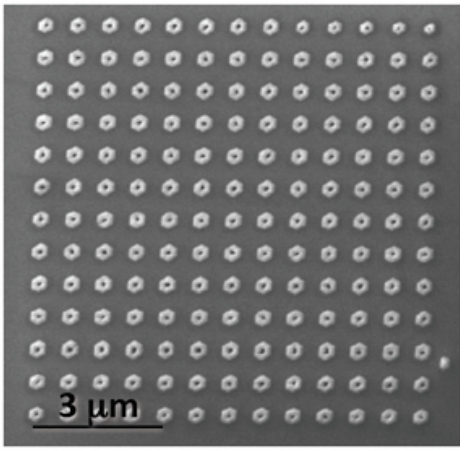

Figure 15 – Array of 300 nm diameter GaN nanorod seeds grown by selective OMVPE in a template patterned by FIB. The array pitch is 750 nm. Note that each nanopyramid seed in this array contains a central nanopore that is filled in upon further growth [Wildeson09b], yielding a dislocation free nanopyramid seed. The proposed design will feature similar arrays with hexagonal symmetry pattered by NIL.

Recommendations for future work are highlighted below.

Increase the pitch and uniformity of the nanopyramid arrays: To eliminate the possibility of impingement defects, it will be necessary to increase the regularity of the pattern and the pattern pitch, as can be expected to be achieved with nanoimprint lithography (NIL). Figure 15 shows an example of a regular nanorod/nanopyramid array produced at Purdue by FIB. NIL is expected to yield similar results, but at the

wafer scale using processes that are already well developed for photonic lattice patterning in commercial high-brightness LEDs. To optimize the nanopyramid arrays for LEDs, the pitch should be 500-600 nm, and the pore opening should be in the range of 150-250 nm (maximum diameter that still ensures that threading dislocations are rejected). These dimensions will result in a quantum well area that is ~50% of the total projected area. Strain relaxation and reduced polarization effects are expected to allow increased quantum well thicknesses, which will yield a total (In,Ga)N volume per unit projected area that is comparable to or greater than that achieved in today's planar LEDs

Separate the defect PL from the bandgap PL for the measurement of IQE: The nanopyramid geometry is promising for enhancing the IQE and EQE of deep green LEDs beyond what has been achieved in planar LEDs to date. Strain relaxation, reduced electric fields in the semipolar quantum wells, and the opportunity to introduce and tune apex quantum dots all contribute towards greater potential at the longer wavelengths. A particular challenge that must be addressed is the accurate measurement of IQE. The PL ratio method is simple, but does not include the effects of applied electric fields, nor does it account for the possibility that the 4K IQE is substantially below 100% for heterostructures with peak emission wavelengths beyond about 500 nm [Hangleiter04;Laubsch09]. The results of the present study are consistent with prior work by others [Wang09], suggesting that Ga vacancies or related defect complexes that are "exposed" in depleted near-surface regions of GaN nanorods or nanowires give rise to yellow PL with a weak temperature dependence [Reshchikov01]. Thus, to understand the phenomena limiting IQE at green and longer wavelengths, it will be necessary to separate the defect luminescence from the (In,Ga)N bandgap (or near-bandedge) luminescence by studying temperature, time and bias dependencies. This recommendation applies to any approach to green gap luminescence in (In,Ga)N heterostructures. The nanopyramid heterostructures developed in this SSL project, however, represent nearly ideal testbeds for such studies, as they are free of dislocations, and can be tuned to luminesce across the entire visible spectrum.

Utilize EL to extract IQE: In addition to the analysis of PL, it will be necessary to compare with EL-based methods for extraction of IQE. One EL method that is both more relevant to devices than PL, and reasonably simple to implement, is the EL decay method of Saito et al. [Saito08]. A model of nonradiative and radiative recombination rates is necessary for extracting IQE from the EL decay characteristics. Unfortunately, a model that includes leakage and Auger effects is probably too complex to allow for unambiguous extraction of IQE with this method.

The most rigorous and direct method for IQE extraction from EL requires modeling of the extraction efficiency, χ. In planar LEDs, methods to estimate χ are complex but tractable [Laubsch09;Getty09]. A calculation of χ for a nanopyramid, or an array of nanopyramids, will likely require a full-wave analysis that accounts for diffraction effects, the details of the polarization of light emitted from the quantum well and apex quantum dot sources, and the complex spatial dependence of the indices of refraction. Metallic contacts present a special challenge because of the potential for plasmonic effects that could significantly impact light extraction. Future work should employ this full-wave analysis approach.

The EL approach to extracting IQE also has the advantage that it is amenable to studies of efficiency droop, a necessary aspect of any research plan aiming to understand and enhance IQE at emission wavelengths in the green gap.

Focus on 540 nm: In concert with the current Multi-Year Project Plan (MYPP09), future work on nanopyramid array LEDs should focus on the goal of 90% IQE at 540 nm. This achievement, combined with more modest improvements in the red and blue, would form the foundation for an efficient white source based on color mixing. The recently completed SSL project demonstrated an IQE by the PL

method of ~10% at ~600 nm. A significantly higher IQE would be expected at 540 nm. However, any such measurements should be validated by more device-relevant EL based methods as discussed above.

To reach the goal of a 69% efficient color-mixed LED package efficiency, it will be necessary to engineer the band offsets in the 540 nm heterostructure, even with an IQE of 90% and an EQE of 81% as targeted in the MYPP. In particular, the conduction band offset between a GaN electron injection layer and the (In,Ga)N recombination volume must be reduced to minimize the energy lost to heat as the electron thermalizes to the lowest available state in the (In,Ga)N recombination region. Thus, it will also be necessary to employ (In,Ga)N alloys for the electron injection layer, perhaps utilizing doping and tunneling barriers to preserve sufficient confinement of holes in the recombination volume. Patterned micro- and nanostructures are expected to facilitate the strain relaxation necessary to grow uniform (In,Ga)N layers with InN mole fractions in the range of 0.1 to 0.15, as would be appropriate for electron injection into recombination volumes with higher InN mole fractions.

A direct LED source at 540 nm would form the basis for developing an integrated white light source based on color mixing, with the goal of reducing the packaging costs and simplifying the optics of the luminaire.

D. References Cited

Chen YS, Shiao W-Y, Tang T-Y, Chang W-M, Liao C-H, Lin C-H, Shen K-C, Hsu M-C, Yeh J-H, Hsu T-C (2009) Threading dislocation evolution in patterned GaN nanocolumn growth and coalescence overgrowth, J Appl Phys 106: 023521

Chichibu SF, Uedono A, Onuma T, Haskell BA, Chakraborty A, Koyama T, Fini PT, Keller S, DenBaars SP, Speck JS, Mishra UK, Nakamura S, Yamaguchi S, Kamiyama S, Amano H, Akasaki I, Han J, Sota T (2006) Origin of defect-insensitive emission probability in In-containing (Al,In,Ga)N alloy semiconductors, Nature Materials 5: 810-16

Colby R, Liang Z, Wildeson I, Sands TD, García RE, Stach EA (2009) Dislocation filtering in GaN nanostructures demonstrated by transmission electron microscopy and numerical analysis, to be submitted to Nano Letters

Deb P, Kim H, Rawat V, Oliver M, Kim S, Marshall M, Stach E, Sands T (2005) Faceted and Vertically Aligned GaN Nanorod Arrays Fabricated without Catalysts or Lithography, Nano Letters, **5**: 1847-51

Getty A, Matioli E, Iza M, Weisbuch C, Speck JS (2009) Electroluminescent measurement of internal quantum efficiency of light emitting diodes, Applied Physics Letters 94: 181102-4

Hangleiter A, Fuhrmann D, Grewe M, Hitzel F, Klewer G, Lahmann S, Netzel C, Riedel N, Rossow U (2004) Towards understanding the emission efficiency on nitride quantum wells, Physica Status Solidi (a) 201: 2808-13

Laubsch A, Sabathil M, Bergbauer W, Strassburg M, Lugauer H, Peter M, Lutgen S, Linder N, Streubel K, Hader J, Moloney JV, Bernhard P, Koch SW (2009) On the origin of IQE-'droop' in InGaN LEDs, Physica Status Solidi (c) 6: 5913-16

Liang Z, Colby R, Garcia RE, Stach EA (2009) Modeling of Dislocation Free Nanostructured InGaN-Based Light Emitting Diodes, to be submitted to the J Appl Phys.

Majewski JA, Vogl P (1998) Polarization and band offsets of stacking faults in AlN and GaN, MRS Internet J. Nitride Semicond. Res. 3: 21

MYPP09, Multi-Year Program Plan FY'09-FY'15, Solid-State Lighting Research and Development, March 2009 (available at www.ssl.energy.gov)

Oliver MH, Schroeder JL, Ewoldt DA, Wildeson IH, Rawat V, Colby R, Cantwell PR, Stach EA, Sands TD (2008) Organometallic vapor phase epitaxial growth of GaN on ZrN/AlN/Si substrates, Appl Phys Lett 93: 023109-3

Park SH, Ahn D (2007) Depolarization effects in (11-22)-oriented InGaN/GaN quantum well structures, Applied Physics Letters **90**: 013505-7

Pérez-Solórzano V, Gröning A, Jetter M, Riemann T, Christen J (2005) Near-red emission from site-controlled pyramidal InGaN quantum dots, Appl Phys Lett 87: 163121

Reshchikov MA, Korotkov RY (2001) Analysis of the temperature and excitation intensity dependencies of photoluminescence in undoped GaN films, Phys Rev B 64: 115205-11

Saito S, Narita T, Zaima K, Tachibana K, Nago H, Hatakoshi G, Nunoue S (2008) Estimation of internal quantum efficiency in InGaN-based light emitting diodes using electroluminescence decay times, Physica Status Solidi (c) 5: 2195-7

Wang G, Li Q, Talin AA, Armstrong A, Lin Y, Huang J (2009) GaN Nanowires: Growth, Characterization, and Applications, ECS Transactions 19: 55-61

Wildeson I, Colby R, Ewoldt D, Zakharov D, Stach E, Sands T (2009a) III-nitride nanopyramid LEDs grown by organometallic vapor phase epitaxy, in preparation.

Wildeson I, Ewoldt D, Colby R, Stach E, Sands T (2009b) Controlled growth of ordered nanopore arrays with GaN nanorods, to be submitted to Journal of Vacuum Science and Technology B

Zang K, Wang Y, Chua SJ (2009) Low dimensional nanostructured InGaN multi-quantum wells by selective area heteroepitaxy, Phys. Status Solidi C 6: S514-S518

Zhong H, Tyagi A, Fellows NN, Wu F, Chung RB, Saito M, Fujito K, Speck JS, DenBaars SP, Nakamura S (2007) High power and high efficiency blue light emitting diode on freestanding semipolar $(10\bar{1}\bar{1})$ bulk GaN substrate, Appl Phys Lett 90: 233504-6

E. Products

E.1. Publications citing support under DE-FC26-06NT42862

H.G. Kim, P. Deb and T. Sands, "High-reflectivity Al-Pt Nanostructured Ohmic Contact to p-GaN," *IEEE Transactions on Electron Devices* **53** (2006) pp. 2448-53.

P. Deb, H. Kim, Y. Qin, R. Lahiji, M. Oliver, R. Reifenberger and T. Sands, "GaN nanorod Schottky and p-n junction diodes," *Nano Letters* **6** (2006) pp. 2893-8.

H. Kim, P. Deb, and T. Sands, "Nanopatterned Contacts to GaN," *J. Electronic Mater.* **36** (2007) pp. 359-67.

P. Deb, T. Westover, H. Kim, T. Fisher and T. Sands, "Field emission from GaN and (Al,Ga)N/GaN nanorod heterostructures," *J. Vac. Sci. Technol. B* **25** (2007) pp. L15-18.

S. Kim, J.L. Schroeder and T.D. Sands, "Pulsed Selective Growth of Hexagonal GaN Microprisms," *J. Crystal Growth*, **310** (2008) pp. 1107-11.

M.H. Oliver, J.L. Schroeder, D.A. Ewoldt, I.H. Wildeson, V. Rawat, R. Colby, P.R. Cantwell, E.A. Stach and T. D. Sands, "Organometallic Vapor Phase Epitaxial Growth of GaN on ZrN/AlN/Si Substrates," *Appl. Phys. Lett.* **93** (2008) 023109.

R. Colby, Z. Liang, I.H. Wildeson, T. Sands, R.E. García, and E.A. Stach, "Dislocation filtering in GaN nanostructures demonstrated by transmission electron microscopy and numerical analysis," to be submitted to *Nano Letters,* 2009.

Z. Liang, R. Colby, R.E. Garcia, and E.A. Stach "Modeling of Dislocation Free Nanostructured InGaN-Based Light Emitting Diodes," (2009) to be submitted to J. Appl. Phys.

I. Wildeson, D. Ewoldt, R. Colby, E.A. Stach, T.D. Sands, "Controlled growth of ordered nanopore arrays with GaN nanorods," (2009) to be submitted to Journal of Vacuum Science and Technology B.

S. Kim, P.R. Cantwell, R. Colby, E.A. Stach, V.P.Drachev and T.D. Sands, "Effect of Hexagonal Prism Cavity on the Electroluminescence from Blue GaN Light Emitting Diodes." (2009) to be submitted.

I. Wildeson, R. Colby, D. Ewoldt, D. Zakharov, E.A. Stach, and T.D. Sands "III-nitride nanopyramid LEDs grown by organometallic vapor phase epitaxy," (2009) in preparation.

E.2. Invited Talks

"Nanoheteroepitaxy: An approach toward a monolithic phosphor-free white LED," T.D. Sands, Nanomaterials Symposium, TMS 2008, New Orleans, LA, March 10th, 2008.

"Nanoheteroepitaxy: An Approach Toward Phosphor-free Monolithic White LEDs," T.D. Sands, IMEC, Leuven, Belgium, May 15th, 2007.

"InGaN-based Nanostructures for High-Performance Light Emitting Devices," R.E. Garcia, T.D. Sands and E.A. Stach, Amer. Soc. Ceramics Meeting; presented by R.E. Garcia in Daytona Beach, FL, Jan. 21st, 2008.

"Nanoheteroepitaxy: An Approach Toward a Monolithic, Phosphor-free White LED," Joint India-US Workshop on Scalable Nanomaterials for Enhanced Enery Transport, Conversion and Efficiency, J.F. Welch Technology Centre, GE Global Research, Bangalore, India, August 21st, 2008.

"Towards Yellow-Green Nanostructured LEDs on Metallized Silicon Substrates," T.D. Sands, Philips LumiLEDS Lighting, San Jose, CA, May 19th, 2009.

E.3. Contributed Presentations

"Nanopatterned Contacts to GaN," H. Kim, P. Deb and T. Sands, 2006 Electronic Materials Conference, State College, PA, June 30th, 2006, presented by H. Kim.

"Schottky, p-n Junction and Light-emitting Diodes Employing (In,Ga)N Nanorod Heterostructures," P. Deb, H. Kim, Y. Qin, R. Lahiji, M. Oliver, R. Reifenberger and T. Sands, 2007 MRS Spring Meeting, San Francisco, CA, April 10th, 2007, presented by P. Deb (P. Deb was awarded the MRS Graduate Student Silver Award).

"Nitride Nanorod Arrays for Phosphor-free White LEDs," by P. Deb, H. Kim, D. Ewoldt, M. Oliver, Z. Liang, R.E. Garcia, E.A. Stach and T. Sands, 2007 Electronic Materials Conference, South Bend, IN; presented by T. Sands, June 20th, 2007.

Tutorial - "Solid-State Lighting: An Opportunity for Nanotechnologists to Address the Energy Challenge," T. Sands, NCN Nanotechnology 501 tutorial, presented April 4th, 2007 (on the web at https://www.nanohub.org/resources/2647/).

"Characterization of InGaN Nanorod-based LEDs by Transmission Electron Microscopy," R. Colby, D.N. Zakharov, I.H. Wildeson, D.A. Ewoldt, Z. Liang, E.R. Garcia, T.D. Sands and E.A. Stach, HH4.4, 2009 MRS Spring Meeting, San Francisco, CA, April 15th, 2009, presented by B. Colby.

"Modeling and Design of Dislocation-free Nanostructured InGaN-based Light Emitting Devices," Z. Liang, R. Colby, D. Zakharov, I. Wildeson, R.E. Garcia, E. Stach and T. Sands, AA1.10, 2009 MRS Spring Meeting, San Francisco, CA, April 14th, 2009, presented by Z. Liang.

"InGaAlN Nanorod LEDs with Green Electroluminescence," I. H. Wildeson, D.A. Ewoldt, R. Colby, Z. Liang, D.N. Zakharov, R.E. Garcia, E.A. Stach and T.D. Sands, O2.3, 2009 MRS Spring Meeting, San Francisco, CA, April 14th, 2009, presented by I. Wildeson.

"Low-Cost Substrates for High-Performance Nanorod Array LED," I. Wildeson, R. Colby, Z. Liang, D. Ewoldt, M.H. Oliver, D. Zakharov, J.L. Schroeder, P.R. Cantwell, R.E. Garcia, E.A. Stach and T.D. Sands, poster presented at the 2009 Frontiers in Scalable Nanostructured Materials and Interfaces Workshop: A US-India Joint Workshop, West Lafayette, IN, March 2009.

"Characterizing High-performance Nanorod-array LEDs " Presented at April 2009 DOE/BES Review of the Electron Microscopy Center at Argonne National Laboratory, R. Colby, I. H. Wildeson, D. A. Ewoldt, Z. Liang, D. N.Zakharov, P. Deb, M. Oliver, R. Edwin Garcia, E. A. Stach, T. D. Sands and N. J. Zaluzec.

"OMVPE Growth and Characterization of III-Nitride Nanorod LEDs," I.H. Wildeson, D.A. Ewoldt, R. Colby, Z. Liang, D.N. Zakharov, R.E. Garcia, E.A. Stach and T.D. Sands, 2009 Electronic Materials Conference, June 2009, State College, PA.

E.4. Inventions and Patent Applications

Invention Disclosure, "Phosphor-free InGaN White LED." Parijat Deb, Ho Gyoung Kim and T. Sands, submitted to OTC, Dec. 2006; Status: did not pursue due to conflicting prior art.

Provisional Patent Application, "Metalized Silicon Substrate for Indium Gallium Nitride Light-Emitting Diode," Timothy D. Sands, Mark H. Oliver, Jeremy L. Schroeder and Vijay Rawat, Application 61/045,116, filed April 15th, 2008; Second Provisional 61/051,950 filed May 9th, 2008; converted to US

utility application and PCT on April 15th, 2009; Status: interest expressed by AMAT, Philips and 3M, as well as a large number on non-NGLIA companies and VCs; not yet licensed.

Invention Disclosure, "Growth Process for Gallium Nitride (GaN) Porous Nanorods," Isaac Wildeson and Timothy D. Sands, submitted to OTC, May 2009; Status: pending; no obvious relationship to SSL.